http://doi.org/10.1093/plphys/kiab571 PLANT PHYSIOLOGY 2022: 188: 2228–2240

Plant Physiology®

Research Article

Type 2C protein phosphatase clade D family members dephosphorylate guard cell plasma membrane H^+-ATPase

Mitsumasa Akiyama,[1] Hodaka Sugimoto,[1] Shin-ichiro Inoue,[1] Yohei Takahashi,[1] Maki Hayashi,[1] Yuki Hayashi,[1] Miya Mizutani,[1] Takumi Ogawa,[1] Daichi Kinoshita,[1] Eigo Ando ,[1] Meeyeon Park ,[2] William M. Gray [2] and Toshinori Kinoshita [1,3,*,†]

1 Division of Biological Science, Graduate School of Science, Nagoya University, Chikusa, Nagoya 464-8602, Japan
2 Department of Plant and Microbial Biology, University of Minnesota, St. Paul, Minnesota 55108, USA
3 Institute of Transformative Bio-Molecules (WPI-ITbM), Nagoya University, Chikusa, Nagoya 464-8602, Japan

*Author for correspondence: kinoshita@bio.nagoya-u.ac.jp
†Senior author.

These authors contributed equally (M.A., H.S.).

S.I., W.M.G., and T.K conceived research plans; S.I. and T.K. supervised the experiments; M.A., H.S., S.I., M.H., Y.H., Y.T., M.M., T.O., D.K., E.A., M.P., and T.K. performed the experiments and analyzed the data; S.I., Y.H., Y.T., M.M., E.A., W.M.G., and T.K. wrote the article.

The author responsible for distribution of materials integral to the findings presented in this article in accordance with the policy described in the Instructions for Authors (https://academic.oup.com/plphys/pages/general-instructions) is: Toshinori Kinoshita (kinoshita@bio.nagoya-u.ac.jp).

Abstract

Plasma membrane (PM) H^+-ATPase in guard cells is activated by phosphorylation of the penultimate residue, threonine (Thr), in response to blue and red light, promoting stomatal opening. Previous in vitro biochemical investigation suggested that Mg^{2+}- and Mn^{2+}-dependent membrane-localized type 2C protein phosphatase (PP2C)-like activity mediates the dephosphorylation of PM H^+-ATPase in guard cells. PP2C clade D (PP2C.D) was later demonstrated to be involved in PM H^+-ATPase dephosphorylation during auxin-induced cell expansion in Arabidopsis (*Arabidopsis thaliana*). However, it is unclear whether PP2C.D phosphatases are involved in PM H^+-ATPase dephosphorylation in guard cells. Transient expression experiments using Arabidopsis mesophyll cell protoplasts revealed that all PP2C.D isoforms dephosphorylate the endogenous PM H^+-ATPase. We further analyzed PP2C.D6/8/9, which display higher expression levels than other isoforms in guard cells, observing that *pp2c.d6*, *pp2c.d8*, and *pp2c.d9* single mutants showed similar light-induced stomatal opening and phosphorylation status of PM H^+-ATPase in guard cells as Col-0. In contrast, the *pp2c.d6/9* double mutant displayed wider stomatal apertures and greater PM H^+-ATPase phosphorylation in response to blue light, but delayed dephosphorylation of PM H^+-ATPase in guard cells; the *pp2c.d6/8/9* triple mutant showed similar phenotypes to those of the *pp2c.d6/9* double mutant. Taken together, these results indicate that PP2C.D6 and PP2C.D9 redundantly mediate PM H^+-ATPase dephosphorylation in guard cells. Curiously, unlike auxin-induced cell expansion in seedlings, auxin had no effect on the phosphorylation status of PM H^+-ATPase in guard cells.

Received September 21, 2021. Accepted November 5, 2021. Advance access publication December 11, 2021

Introduction

Stomata in the epidermis regulate gas exchange for controlling of CO_2 uptake for photosynthesis and transpiration for nutrient uptake in roots. Various environmental signals are known to affect stomatal movements. Among them, it is well studied that stomatal opening is stimulated by light, including blue and red light (Shimazaki et al., 2007; Inoue and Kinoshita, 2017). Blue light-induced stomatal opening is mediated by blue-light photoreceptor phototropins (phot1 and phot2) through the activation of plasma membrane (PM) H^+-ATPase (Kinoshita et al., 2001; Doi et al., 2004). PM H^+-ATPase is activated by the phosphorylation of a penultimate threonine (Thr) residue in the C-terminal auto-inhibitory domain, and subsequent binding of 14-3-3 proteins to the phosphorylated C-terminus of PM H^+-ATPase in guard cells within 30 s after blue light treatment (Kinoshita and Shimazaki, 1999; Ueno et al., 2005; Hayashi et al., 2011). The resulting increase in PM H^+-ATPase activity hyperpolarizes the PM and provides the driving force for stomatal opening (Toda et al., 2016; Yamauchi et al., 2016). It has been reported that the BLUE LIGHT SIGNALING1 (BLUS1; Takemiya et al., 2013) and BLUE LIGHT-DEPENDENT H^+-ATPASE PHOSPHORYLATION (BHP; Hayashi et al., 2017) protein kinases, and a type 1 protein phosphatase (Takemiya et al., 2006) have important roles in the BLUS pathway between phototropins and PM H^+-ATPase activation in guard cells. More recently, Ando and Kinoshita (2018) showed that red light also induces phosphorylation of penultimate Thr of PM H^+-ATPase in guard cells in the photosynthesis-dependent manner and promotes stomatal opening.

Plant PM H^+-ATPase belongs to the P-type family of ATPases. PM H^+-ATPase transports H^+ out of the cell coupled with ATP hydrolysis and so creates an electrochemical gradient across the PM for energizing solute transport (Palmgren, 2001; Falhof et al., 2016). PM H^+-ATPase has structural similarity with Ca^{2+}-ATPase, H^+/K^+-ATPase, and Na^+/K^+-ATPase, belonging to the P-type ATPases, which have 10 transmembrane segments and an N- and C-terminus in the cytosol. In the Arabidopsis (*Arabidopsis thaliana*) genome, 11 isoforms (*AHA1–AHA11*) have been identified. PM H^+-ATPases are involved in diverse physiological responses including phloem loading and unloading, xylem loading and unloading, solute uptake in roots, leaf movement, tip growth, and cell expansion in addition to stomatal opening (Sondergaard et al., 2004; Takahashi et al., 2012; Hayashi et al., 2014; Spartz et al., 2014; Haruta et al., 2015; Toda et al., 2016; Yamauchi et al., 2016; Ren et al., 2018; Toh et al., 2018; Minami et al., 2019).

PM H^+-ATPase activity is regulated by phosphorylation of several sites in the C-terminus (Haruta et al., 2015; Falhof et al., 2016). Among them, the penultimate Thr is the first reported and most studied phosphorylation site. Phosphorylation of this site induces activation of PM H^+-ATPase and is involved in physiological responses, such as light-induced stomatal opening and auxin-induced cell expansion (Palmgren, 2001; Ren and Gray, 2015; Inoue and Kinoshita, 2017). However, the protein kinase responsible for the phosphorylation of the penultimate Thr residue of PM H^+-ATPase has not been identified, although in vitro protein kinase activity for this site was reported (Svennelid et al., 1999; Hayashi et al., 2010). On the other hand, it has been reported that the dephosphorylation of the phosphorylated penultimate Thr residue of PM H^+-ATPase is mediated by the Mg^{2+}/Mn^{2+}-dependent membrane-localized type 2C protein phosphatase (PP2C)-like activity in broad bean (*Vicia faba*) guard cells and etiolated seedlings in Arabidopsis (Hayashi et al., 2010). Later, PP2C clade D(PP2C.Ds) isoforms were shown to be involved in the dephosphorylation of PM H^+-ATPase in the auxin-induced hypocotyl elongation and cell expansion (Schweighofer et al., 2004; Spartz et al., 2014; Ren and Gray, 2015).

PP2Cs are evolutionarily conserved from prokaryotes to higher eukaryotes and are considered to be active as monomers. Plants possess a large number of PP2Cs compared to mammals. In Arabidopsis, 80 genes are reported to belong to PP2C family and are divided into 10 clades (from A to J; Schweighofer et al., 2004; Xue et al., 2008). Among them, clade D includes nine isoforms, *PP2C.D1–D9*. Each *PP2C.D* displays their own expression pattern and subcellular localization (Tovar-Mendez et al., 2014; Ren et al., 2018). In addition, *SMALL AUXIN-UP RNAs* (*SAURs*), a large multigene family of early auxin-responsive genes, have been shown to inhibit PP2C.D activity through physical interaction (Spartz et al., 2014; Sun et al., 2016). It is noteworthy that *SAUR19*-overexpressing plants displayed enhanced water loss in detached leaves, wilted faster than the wild-type upon cessation of watering, and exhibited delayed stomatal closure (Spartz et al., 2014, 2017). These results suggest that PP2C.Ds might also be involved in PM H^+-ATPase dephosphorylation in guard cells. Very recently, Wong et al. (2021) reported that *PP2C.D2*, *PP2C.D5*, and *PP2C.D6* mediate the control of stomatal movements. However, phosphorylation status of PM H^+-ATPase in guard cells was not investigated.

In the present study, to identify the protein phosphatase involved in the direct dephosphorylation of penultimate Thr residue of PM H^+-ATPase in guard cells, we selected the *PP2C.D6* and *PP2C.D9* isoforms, which show comparatively high expression levels in guard cells, and examined their function in guard cells of Arabidopsis. Our findings indicated that PP2C.D6 and PP2C.D9 redundantly mediate the dephosphorylation of the penultimate Thr residue of PM H^+-ATPase in guard cells.

Results

Dephosphorylation of PM H^+-ATPase by PP2C.D isoforms in mesophyll cell protoplasts

It has been reported that PP2C.Ds mediate the dephosphorylation of the penultimate Thr residue of PM H^+-ATPase in Arabidopsis seedlings (Spartz et al., 2014; Ren et al., 2018). To investigate specificity of PP2C.D isoforms, from PP2C.D1

to PP2C.D9, for the dephosphorylation of PM H^+-ATPase in vivo, we performed transient *PP2C.D* expression assays using Arabidopsis mesophyll cell protoplasts (MCPs) and investigated penultimate Thr phosphorylation status of the endogenous PM H^+-ATPase in MCPs (Figure 1). The phosphorylated PM H^+-ATPase was observed in MCPs when green fluorescent protein (GFP) alone was expressed as a control. In contrast, the expression of *PP2C.D* isoforms, *PP2C.D1–PP2C.D9*, in MCPs as GFP fusion proteins induced the dephosphorylation of the endogenous PM H^+-ATPase without affecting PM H^+-ATPase protein levels. These results clearly indicate that all PP2C.D isoforms can decrease phosphorylation level of the penultimate Thr residue of PM H^+-ATPase in vivo when overexpressed in MCPs. Note that the expressed PP2C.Ds showed two major bands in MCPs. Based on molecular weight predictions, the upper bands likely represent mature GFP-PP2C.D fusion proteins, while the lower bands are presumably truncated synthesis or degradation products.

To examine PP2C specificity, we conducted similar assays where representative members of each of the nine PP2C clades, *PP2C.A* to *PP2C.I*, were transiently expressed in MCPs. As shown in Supplemental Figure S1, only the PP2C.D clade isoform induced the dephosphorylation of the endogenous PM H^+-ATPase in MCPs, although the expression level of each isoform varied. We quantified reduction of phosphorylation level of PM H^+-ATPase based on the expression level of PP2Cs. The result showed that PP2C.D9 effectively dephosphorylated PM H^+-ATPase in MCPs. These results suggest that PP2C.D proteins are likely to specifically dephosphorylate PM H^+-ATPase in vivo.

Expression of *PP2C.D* isoforms in guard cells

To identify the *PP2C.D* isoforms expressed in stomatal guard cells, we analyzed the Arabidopsis eFP Browser database (https://bar.utoronto.ca/efp/cgi-bin/efpWeb.cgi), and found that *PP2C.D9* and *PP2C.D6* are major isoforms in guard cells in transcriptional inhibitors-treated guard-cell protoplasts (GCPs; Winter et al., 2007; Yang et al., 2008; Figure 2A). *PP2C.D9* and *PP2C.D6* comprised around 38% and 28% of the total PP2C.D transcripts, respectively. *PP2C.D2* and *PP2C.D3* were third and fourth most highly expressed isoforms in guard cells, showing 7.8% and 7.2% expression, respectively, and *PP2C.D5* was the fifth most abundant isoform. *PP2C.D6* is ubiquitously expressed in the seedlings in addition to guard cells. In contrast, *PP2C.D9* shows relatively specific expression in guard cells (Supplemental Figure S2; Ren et al., 2018). We further confirmed the published RNAseq data from GCPs and found that *PP2C.D8* also showed higher expression level in guard cells in addition to *PP2C.D6* and *PP2C.D9* (Aoki et al., 2019; Supplemental Table S1). To confirm the expression of *PP2C.D6*, *PP2C.D8*, and *PP2C.D6* in guard cells, we examined GUS (β-glucuronidase) reporter assay using the native *PP2C.D6*, *PP2C.D8*, and *PP2C.D6* promoters (Ren et al., 2018). All *PP2C.D* genes were clearly expressed in stomatal guard cells (Figure 2B).

To study the subcellular localization of PP2C.D6, PP2C.D8, and PP2C.D9, the *PP2C.D6*, *PP2C.D8*, and *PP2C.D9* genes were fused to *GFP* and transiently expressed in broad bean guard cells by particle bombardment (Figure 2C). GFP expression was detected in the cytoplasm and nucleus. GFP-PP2C.D6 and GFP-PP2C.D9 were localized in the peripheral region and cytoplasm of guard cells. On the other hand, GFP-PP2C.D8 was mainly localized in small organelle of guard cells as previously reported (Figure 2C; Ren et al., 2018). To investigate the subcellular localization of PP2C.D9 in more detail, we generated *GFP-PP2C.D9* overexpressing plants under control of guard cell strong promoter *GC1*. As shown in Supplemental Figure S3, GFP-PP2C.D9 were detected in the peripheral region and cytoplasm of guard

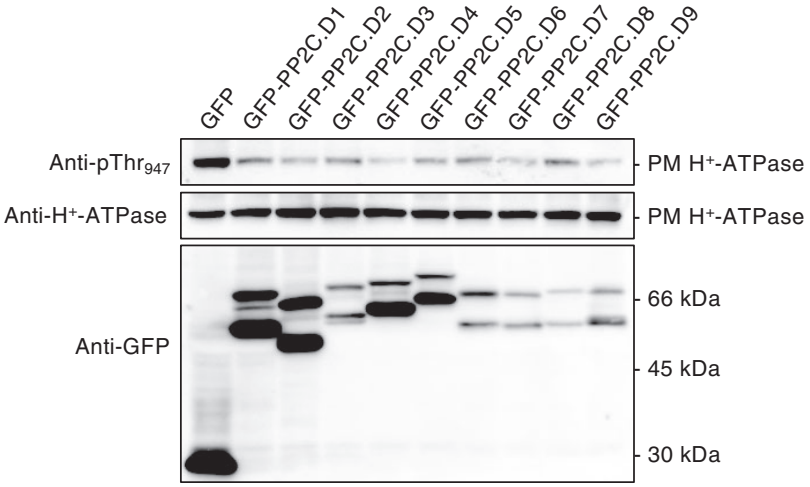

Figure 1. Effect of transiently expressed PP2C.Ds on phosphorylation status of PM H^+-ATPase in MCPs. Arabidopsis MCPs transiently expressing GFP-tagged PP2C.Ds were incubated in incubation buffer at room temperature for 14 h. The phosphorylated PM H^+-ATPase and amount of PM H^+-ATPase were detected by immunoblot using anti-phospho-Thr947 antibody (Anti-$pThr_{947}$) and a specific antibody for PM H^+-ATPase (anti-H^+-ATPase), respectively. GFP-tagged PP2C.Ds were detected by immunoblot using the anti-GFP antibody. Numbers on the right side represent the positions of molecular weight markers.

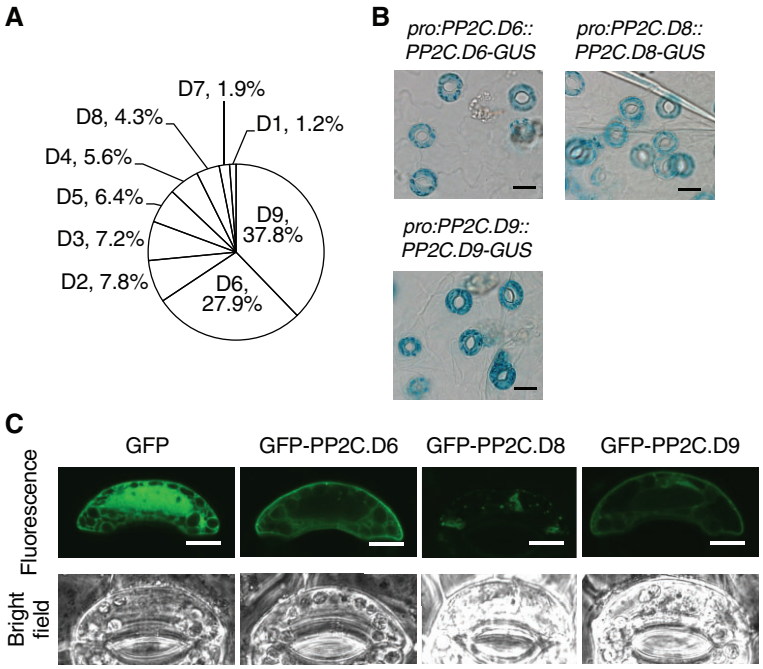

Figure 2. Expression and localization of PP2C.D6, PP2C.D8 and PP2C.D9. A, Relative expression levels of *PP2C.Ds* in transcriptional inhibitors-untreated GCPs. Expression level of each *PP2C.D* was obtained from eFP browser (http://bar.utoronto.ca/efp/cgi-bin/efpWeb.cgi; Yang et al., 2008). B, Expression of *PP2C.D6*, *PP2C.D8* and *PP2C.D9* in the epidermis. The epidermal tissues were obtained from rosette leaves of 4-week-old transgenic plants expressing the *GUS* reporter gene under control of *PP2C.D6* and *PP2C.D9* promoters. GUS staining was performed at 37°C for 16 h. Bars = 10 μm. C, Subcellular localization of PP2C.D6, PP2C.D8, and PP2C.D9. Gene constructs encoding GFP-fused *PP2C.D6* or *PP2C.D8* or *PP2C.D9* under *35SCaMV* promoter were transformed into guard cells of broad bean by particle bombardment. Typical fluorescent images from GFP obtained by a confocal microscope and images of guard cells taken with phase-contrast microscopy are shown. Bars = 10 μm.

cells and co-localized with the fluorescence of the dye FM4–64, a marker labeling the PM.

Stomatal phenotypes in *pp2c.d6*, *pp2c.d8*, and *pp2c.d9* single mutants

To investigate light-induced stomatal opening and blue light-dependent phosphorylation of penultimate Thr residue of the guard-cell PM H^+-ATPase of *PP2C.D6*, *PP2C.D8*, and *PP2C.D9* mutants, we obtained *pp2c.d6*, *pp2c.d8*, and *pp2c.d9* T-DNA insertion mutants (Figure 3A). The transcripts were not detected by reverse transcription–polymerase chain reaction (RT–PCR) in all mutants (Figure 3B), suggesting that *pp2c.d6*, *pp2c.d8*, and *pp2c.d9* single mutants are null alleles. We next investigated light-induced stomatal opening and blue light-dependent phosphorylation of penultimate Thr residue of the guard-cell PM H^+-ATPase by the immunohistochemical method using the antibody against phosphorylated penultimate residue, Thr (anti-pThr_{947} antibody) in the epidermis (Figure 3, C and D; Hayashi et al., 2011). However, all single mutants showed almost similar stomatal responses with background ecotype, Col-0.

Stomatal phenotypes in *pp2c.d6 pp2c.d9* double mutant

Next, we investigated stomatal phenotypes in the *pp2c.d6/9*, *pp2c.d6/8*, and *pp2c.d8/9* double mutants and *pp2c.d6/8/9* triple mutant (Figure 4A). Interestingly, we found that the stomata in *pp2c.d6/9* double mutant opened more widely compared to Col-0 in response to light (Figure 4B). However, stomatal apertures in *pp2c.d6/8* and *pp2c.d8/9* double mutants did not show significant difference compared to those in Col-0 under light condition. In addition, stomatal aperture in *pp2c.d6/8/9* triple mutant was almost comparable to that of *pp2c.d6/9* double mutant, suggesting that PP2C.D6 and PP2C.D9 redundantly mediate regulation of stomatal aperture.

Next, we investigated phosphorylation status of penultimate Thr residue of PM H^+-ATPase in guard cells by the immunohistochemical method (Figure 4C). The phosphorylation level in the *pp2c.d6/9* double mutant was slightly higher than Col-0 under red light condition and significantly higher (50%) at 2.5 min after the start of blue light illumination, without altering the amount of PM H^+-ATPase in guard cells (Supplemental Figure S4). Consistent with the results of stomatal aperture measurements, phosphorylation level of PM H^+-ATPase in *pp2c.d6/8* and *pp2c.d8/9* double mutants were almost similar to those in Col-0.

To further characterize the *pp2c.d6/9* double mutant, we investigated the dephosphorylation kinetics of PM H^+-ATPase in guard cells (Figure 5). In Col-0, phosphorylation level of PM H^+-ATPase decreased by $>60\%$ at 5 min after the start of 30-s blue light pulse. In contrast, in *pp2c.d6/9* double mutant, the phosphorylation level of H^+-ATPase was still over 85% at that time and showed significantly

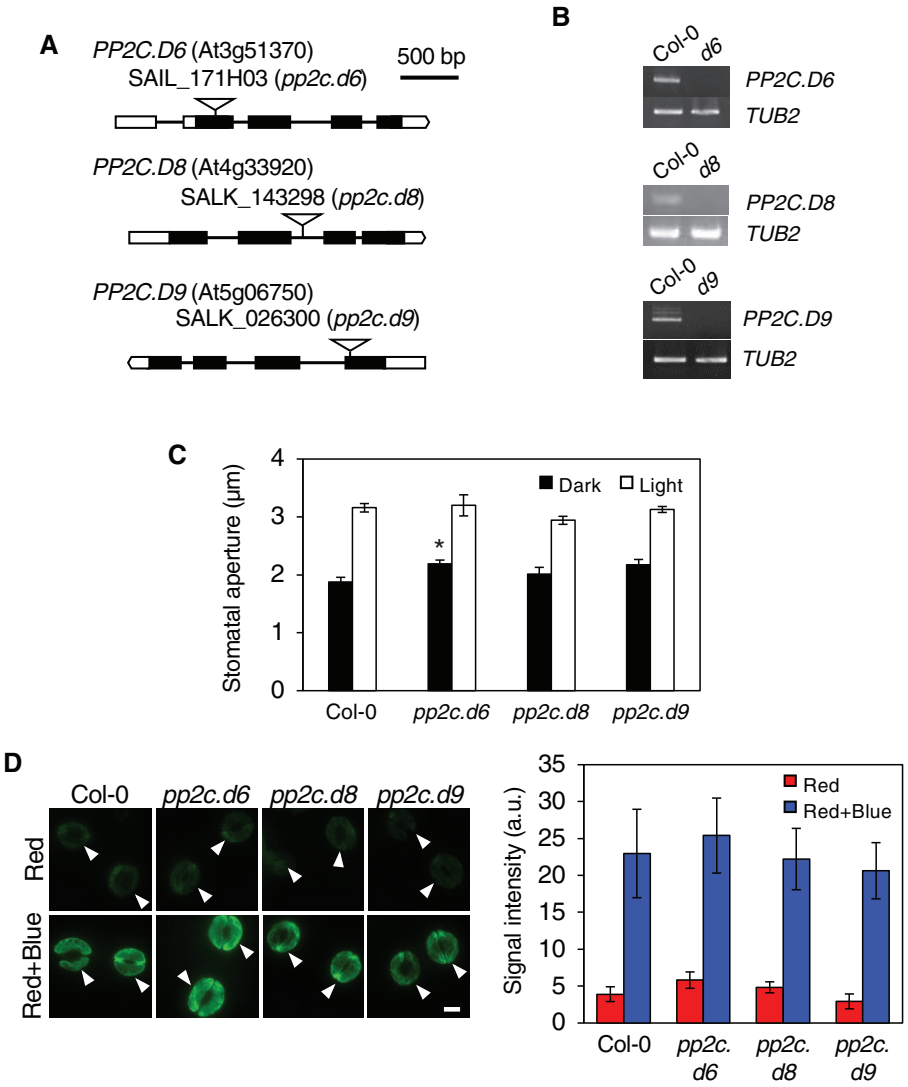

Figure 3. Stomatal phenotypes of *pp2c.d6*, *pp2c.d8*, and *pp2c.d9* single mutants. A, Schematic representation of the structures of *PP2C.D6* (At3g51370), *PP2C.D8* (At4g33920), and *PP2C.D9* (At5g06750) and the location of the T-DNA insertions in *pp2c.d6*, *pp2c.d8*, and *pp2c.d9*. Boxes and lines represent exons and introns, respectively. B, Expression of *PP2C.D6*, *PP2C.D8*, and *PP2C.D9* analyzed by RT-PCR in Col-0, *pp2c.d6*, *pp2c.d8*, and *pp2c.d9*. Total RNA was extracted from rosette leaves of 4-week-old plants. *TUB2* was used as an internal control. C, Stomatal opening in response to light in Col-0, *pp2c.d6*, and *pp2c.d9*. Epidermal tissues from dark-adapted plants in the basal buffer were illuminated with light (blue light at 10 μmol m^{-2} s^{-1} superimposed on red light at 50 μmol m^{-2} s^{-1}) or kept in the dark for 3 h. Values represent mean ± SE (n = 5); measurement of 30 stomata in each experiment. Asterisk indicates statistically significant difference from corresponding Col-0 (Student's t test; *$P < 0.05$). D, Immunohistochemical detection of the phosphorylation of PM H^+-ATPase in response to blue light in Col-0, *pp2c.d6*, *pp2c.d8*, and *pp2c.d9* guard cells. Epidermal tissues from dark-adapted plants were illuminated with red light (50 μmol m^{-2} s^{-1}) for 20 min (Red), after which blue light (10 μmol m^{-2} s^{-1}) was superimposed on the red light for 2.5 min (Red + Blue). The phosphorylated PM H^+-ATPase was detected by the immunohistochemical method using anti-$pThr_{947}$ antibody. Typical fluorescent images (left) and relative intensities of the fluorescent signals (right) are shown. Arrowheads indicate the position of the stomata. Bars = 10 μm. Data indicate mean ± SD (n = 5) with measurement of 30 stomata in each sample.

higher phosphorylation level than Col-0 for over 40 min. The amount of PM H^+-ATPase was unchanged over time in both Col-0 and *pp2c. d6/9* (Supplemental Figure S5). These results indicate that PP2C.D6 and PP2C.D9 redundantly mediate the dephosphorylation of PM H^+-ATPase. Note that the dephosphorylation of PM H^+-ATPase was delayed, but was still observed in the *pp2c.d6/9* double mutant, suggesting that PP2C.D6 and PP2C.D9 are not prominent and other PP2C.Ds are also involved in the dephosphorylation of PM H^+-ATPase in guard cells.

To investigate stomatal phenotypes in more detail, we measured stomatal conductance in intact leaves of *pp2c.d6/9* using a gas-exchange system (Supplemental Figure S6). In Col-0 leaves, stomatal conductance increased after illumination of red light for 1 h and then saturated; the illumination of blue light superimposed on red light-induced rapid increase of the conductance at the first 15 min, then decreased gradually (Supplemental Figure S6B). Stomatal conductance in *pp2c.d6/9* also rapidly increased after the illumination of blue light, whereas did not decrease after

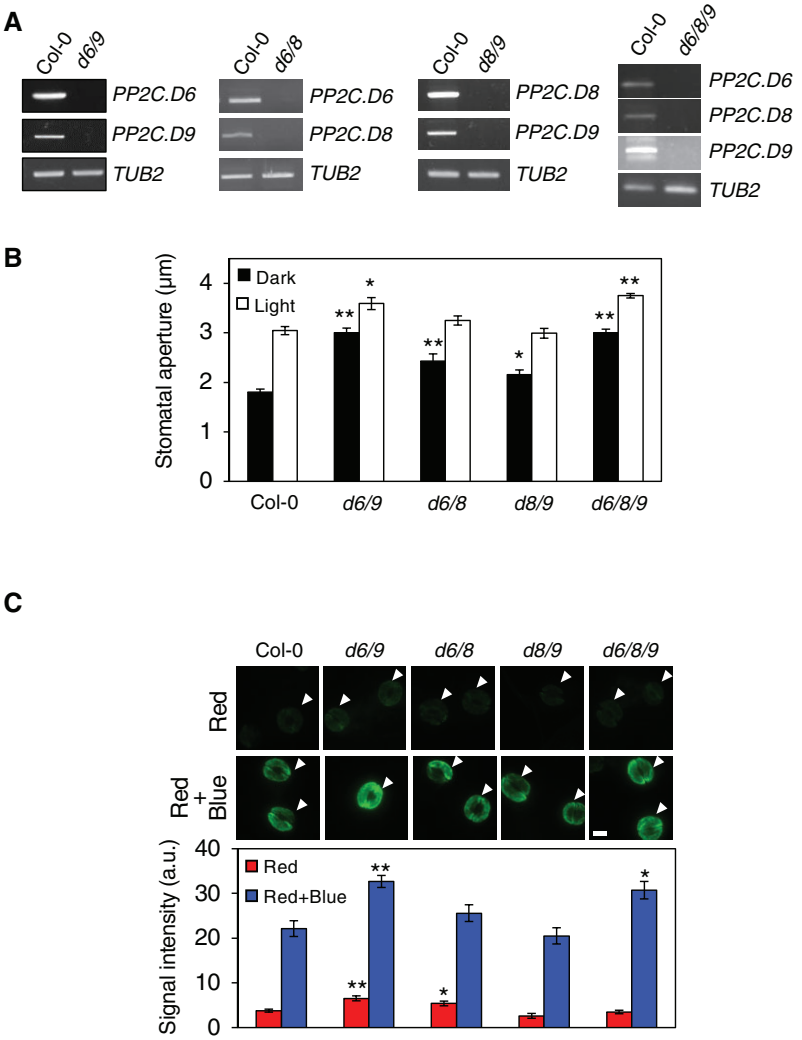

Figure 4. Stomatal phenotypes in *pp2c.d6/9*, *pp2c.d6/8*, and *pp2c.d8/9* double mutants. A, Expression of *PP2C.D6*, *PP2C.D8* and *PP2C.D9* analyzed by RT-PCR in Col-0 and *pp2c.d6/9*, *pp2c.d6/8* and *pp2c.d8/9*. Other details are the same as in Figure 3B. B, Stomatal opening in response to light in Col-0 and *pp2c.d6/9*, *pp2c.d6/8*, *pp2c.d8/9*, and *pp2c.6/8/9*. Other details are the same as in Figure 3C. Asterisk indicates statistically significant difference from corresponding Col-0 (Student's *t* test; $^{*}P < 0.05$, $^{**}P < 0.01$). C, Immunohistochemical detection of the phosphorylation of PM H^+-ATPase in response to blue light in Col-0 and *pp2c.d6/9*, *pp2c.d6/8*, *pp2c.d8/9*, and *pp2c.6/8/9* guard cells. Other details are the same as in Figure 3D. Asterisk indicates statistically significant difference from corresponding Col-0 (Student's *t* test; $^{*}P < 0.05$, $^{**}P < 0.01$).

15 min from start of blue light illumination. Thus, *pp2c.d6/9* showed different kinetics of stomatal conductance after blue light illumination compared to Col-0.

Stomatal aperture in the *pp2c.d6/9* double mutant opened widely not only under light illumination but also in the dark for 3 h (Figure 4B). In contrast, stomatal conductance of *pp2c.d6/9* in the dark was only slightly higher than that of Col-0 (Supplemental Figure S6). Then, we investigated time course of stomatal aperture of *pp2c.d6/9* in the dark. As shown in Supplemental Figure S7, at the beginning of the measurement, stomatal aperture of *pp2c.d6/9* was comparable to that of Col-0, while after 1 h, stomata in *pp2c.d6/9* opened even in the dark. These results suggest that mutation of *pp2c.d6/9* facilitates stomatal opening in the basal buffer for stomatal measurement (see "Materials and Methods").

Stomatal phenotypes in *PP2C.D9* overexpressing plants

To investigate the function of PP2C.D9 in stomatal guard cells, we investigated stomatal phenotype of *PP2C.D9* overexpressing plants (*pGC1:GFP-PP2C.D9*). As shown in Figure 6, stomata in *PP2C.D9* overexpression lines did not open in response to light. This result strongly supports that PP2C.D9 is a negative regulator of light-induced stomatal opening, probably due to enhancement of the dephosphorylation of PM H^+-ATPase.

Direct dephosphorylation of PM H^+-ATPase by PP2C.D9

To confirm the direct dephosphorylation of PM H^+-ATPase by PP2C.D6 and PP2C.D9, we tried to purify the

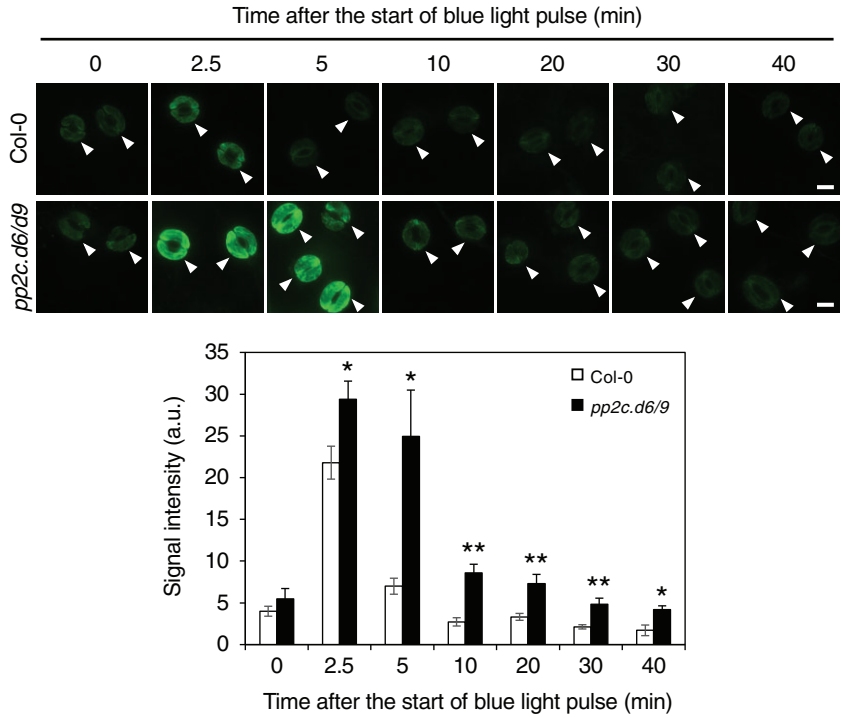

Figure 5. Time course of PM H^+-ATPase dephosphorylation after blue light illumination in Col-0 and *pp2c.d6/9* guard cells. Epidermal tissues from dark-adapted plants were pre-illuminated with red light (50 μmol m^{-2} s^{-1}) for 20 min, then a blue light pulse (10 μmol m^{-2} s^{-1}, 30 s) was superimposed on the red light. The epidermal tissues were fixed at the indicated time points and phosphorylated PM H^+-ATPase was detected by immunohistochemical method. Typical fluorescent images (upper) and relative intensities of the fluorescent signals (lower) are shown. Arrowheads indicate the position of the stomata. Bar = 10 μm. Data indicate mean ± SE (n = 5) with measurement of 30 stomata in each sample. Asterisk indicates statistically significant difference from corresponding Col-0 (Student's t test; *$P < 0.05$, **$P < 0.01$).

recombinant PP2C.D6 and PP2C.D9 proteins from *Escherichia coli*. Unfortunately, we could not obtain recombinant PP2C.D6 protein from *E. coli*; therefore, we performed dephosphorylation assay using only the recombinant PP2C.D9 protein. In this assay, we used PM H^+-ATPase (AHA2) heterologously expressed in yeast as a substrate, which is phosphorylated on penultimate Thr residue in yeast (Maudoux et al., 2000; Spartz et al., 2014; Ren et al., 2018). The results showed that phosphorylated PM H^+-ATPase in the isolated yeast membranes was clearly dephosphorylated by the recombinant PP2C.D9 protein in vitro, but PM H^+-ATPase was not dephosphorylated without the recombinant PP2C.D9 protein (Figure 7).

Auxin had no effect on the phosphorylation status of PM H^+-ATPase in guard cells

During auxin-induced hypocotyl elongation and cell expansion, auxin activates PM H^+-ATPase through the phosphorylation of penultimate Thr residue of PM H^+-ATPase (Takahashi et al., 2012; Uchida et al., 2018). In this process, it has been demonstrated that auxin-induced SAUR proteins directly inhibit PP2C.D phosphatase activity by physical binding to PP2C.D proteins and activate PM H^+-ATPase through the enhancement of phosphorylation level of PM H^+-ATPase (Spartz et al., 2014; Ren et al., 2018). Lohse and Hedrich (1992) showed that auxin induced stomatal opening at optimum concentration 5 μM in broad bean. Later, Tanaka et al. (2006) showed that auxin at 10-μM partially inhibited abscisic acid-induced stomatal closure. To test the effect of auxin on the phosphorylation status of PM H^+-ATPase in guard cells, we treated the epidermis with auxin or the fungal toxin fusicoccin (FC), an activator of PM H^+-ATPase through inhibition of the dephosphorylation of PM H^+-ATPase (Kinoshita and Shimazaki, 2001). As shown in Figure 8, treatment of indole-3-acetic acid (IAA) at 10 μM for 20 min did not induce phosphorylation of PM H^+-ATPase in guard cells. In contrast, FC at 10 μM clearly induced phosphorylation of PM H^+-ATPase. The result indicates that exogenous auxin has no effect on phosphorylation status of the penultimate Thr residue of PM H^+-ATPase in guard cells.

Discussion

In this study, we provide evidence that PP2C.D6 and PP2C.D9 redundantly mediate the dephosphorylation of penultimate Thr residue in the C-terminal auto-inhibitory domain of PM H^+-ATPase in guard cells. We selected *PP2C.D6* and *PP2C.D9* for stomatal assays based on their high relative expression levels in guard cells (Figure 2). Single mutants of *PP2C.D6* and *PP2C.D9* showed normal responses in light-induced stomatal opening and blue light-induced phosphorylation of PM H^+-ATPase (Figure 3). In contrast, the *pp2c.d6/9* double mutant showed an open stomata phenotype under light illumination and a significant delay in

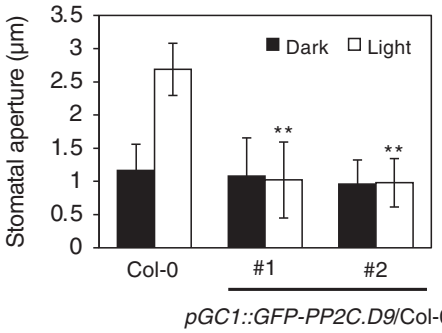

Figure 6. Stomatal opening in response to light in Col-0 and *pGC1::GFP-PP2C.D9*/Col-0. Values represent mean ± SD; measurement of 30 stomata in each experiment. Double asterisk indicates statistically significant difference from corresponding Col-0 (Student's *t* test; $^{**}P < 0.01$). Experiments were repeated on three occasions with similar results. Other details are the same as in Figure 3C.

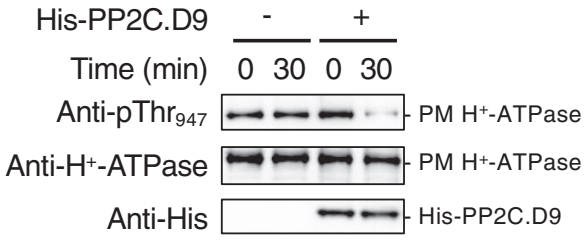

Figure 7. In vitro phosphatase assay using recombinant PP2C.D9 protein for the dephosphorylation of yeast-expressed PM H^+-ATPase (AHA2). Microsomal membrane fractions isolated from yeast expressing AHA2 were used for *in vitro* phosphatase assays. The microsomes were incubated with or without recombinant His-PP2C.D9 for 30 min at 24°C. His-PP2C.D9 was detected by immunoblot using the anti-His antibody.

the dephosphorylation of PM H^+-ATPase after blue light illumination in guard cells (Figures 4 and 5; Supplemental Figure S6), suggesting that PP2C.D6 and PP2C.D9 mediate the dephosphorylation of PM H^+-ATPase in guard cells. It is worthy of note that although the *pp2c.d6/9* double mutant showed a strong phenotype, it still displayed the dephosphorylation of PM H^+-ATPase, suggesting that other PP2C.D isoforms may also be involved in the dephosphorylation of PM H^+-ATPase in guard cells. Further investigations will be needed to clarify the involvement of other isoforms for the dephosphorylation of PM H^+-ATPase in guard cells. Very recently, Wong et al. (2021) showed involvement of *PP2C.D2*, *PP2C.D5*, and *PP2C.D6* in stomatal movements, suggesting that *PP2C.D2* and *PP2C.D5* are additional candidates for the dephosphorylation of PM H^+-ATPase in guard cells.

In the case of cell expansion in Arabidopsis seedlings, the Arabidopsis eFP Browser database indicates that *PP2C.D5*, *PP2C.D2*, and *PP2C.D6* are the highest expressed *PP2C.D* isoforms, comprising around 22%, 19%, and 15% of total *PP2C.D* transcript signals, respectively (Supplemental Figure S8). Consistent with the expression levels of these isoforms, *pp2c.d2/5/6* triple mutant displayed a stronger hypocotyl growth phenotype than *pp2c.d2/5* and *pp2c.d2/6* double mutants (Ren et al., 2018). These results suggest that the expression levels of *PP2C.D* isoforms are likely to reflect their contribution for the dephosphorylation of PM H^+-ATPase in each cell types and tissues.

Transient PP2C expression assays using Arabidopsis MCPs revealed that potentially all PP2C.D isoforms are able to mediate the dephosphorylation of PM H^+-ATPase in plant cells (Figure 1), and the dephosphorylation of PM H^+-ATPase was not observed when we expressed representative members of the other PP2C clades (Supplemental Figure S1), indicating that these assays are a very useful system to examine the involvement of phosphatases in the dephosphorylation of PM H^+-ATPase in vivo. Previous investigations showed that recombinant PP2C.D1, PP2C.D2, and PP2C.D5 proteins directly dephosphorylate phosphorylated penultimate Thr residue of PM H^+-ATPase (AHA2) expressed in yeast in vitro (Spartz et al., 2014; Ren et al., 2018). In the present study, we also provided biochemical evidence of the direct dephosphorylation of phosphorylated PM H^+-ATPase (AHA2) expressed in yeast by PP2C.D9 protein in vitro (Figure 7). These results strongly suggest that PP2C.D isoforms act as phosphatases for the direct dephosphorylation of the penultimate Thr residue in PM H^+-ATPase. We could not obtain the recombinant PP2C.D6 from *E. coli*, probably due to its toxicity. It will be needed to show the direct dephosphorylation of PM H^+-ATPase by PP2C.D6.

It is still unclear that how blue light regulates the phosphorylation status of penultimate Thr residue of PM H^+-ATPase in guard cells. Previous results indicated that blue light-induced phosphorylation of PM H^+-ATPase and FC-induced phosphorylation of PM H^+-ATPase exhibit similar time courses in GCPs from broad bean (Kinoshita and Shimazaki, 1999, 2001). Given that FC activates PM H^+-ATPase through the inhibition of the dephosphorylation of PM H^+-ATPase, and that FC-induced phosphorylation is observed without blue light illumination in guard cells, a protein kinase catalyzing the direct phosphorylation of penultimate residue, Thr, of PM H^+-ATPase may constantly phosphorylate PM H^+-ATPase in guard cells. It would be expected that the blue light signal inhibits PP2C.D phosphatase activity and induces accumulation of phosphorylated PM H^+-ATPase in guard cells. Therefore, it is very important to identify blue light-dependent regulators of PP2C.D6 and PP2C.D9 proteins for understanding of regulation of the phosphorylation status of the penultimate Thr residue of PM H^+-ATPase in guard cells and the signaling pathway of blue light-induced stomatal opening.

It has been demonstrated that auxin-induced SAUR proteins inhibit PP2C.D activity through the direct binding to PP2C.Ds (Spartz et al., 2014; Ren et al., 2018). Recently, Wong et al. (2019) identified a highly conserved, unique motif near the C-terminus of the catalytic domain of PP2C.D proteins that is essential for SAUR binding. Furthermore, single missense mutations within this motif abolish SAUR binding and inhibition of PP2C.D activity by SAUR. Among the

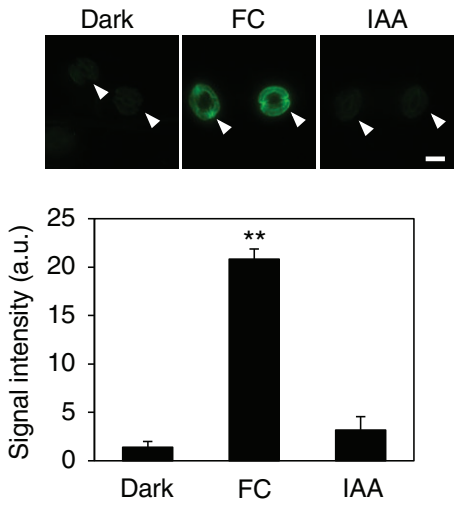

Figure 8. Effect of exogenous auxin on phosphorylation status of PM H^+-ATPase in guard cells. Epidermal tissues from dark-adapted plants were incubated with 0.25% (v/v) DMSO (Dark), 10-μM FC, or 10-μM IAA for 20 min in the dark. FC and IAA were dissolved in DMSO. Typical fluorescent images (upper) and relative intensities of the fluorescent signals (lower) are shown. Arrowheads indicate the positions of the stomata. Bars = 10 μm. Data indicate mean ± SE ($n = 3$) with measurement of 30 stomata in each sample. Double asterisk indicates statistically significant difference from dark sample (Student's t test; $^*P < 0.01$).

top five *PP2C.D* isoforms expressed in guard cells (*PP2C.D9*, *PP2C.D6*, *PP2C.D2*, *PP2C.D3*, and *PP2C.D5*; Figure 2A), only *PP2C.D9* does not conserved the motif completely. It is possible that PP2C.D6, PP2C.D2, PP2C.D3, and PP2C.D5 proteins are also regulated by SAUR protein in guard cells. To support this, GFP- or StrepII-tagged SAUR19 overexpressing Arabidopsis plants showed enhanced water loss in leaf detachment assays and delayed stomatal closure (Spartz et al., 2014). It is possible that PP2C.D9 might not be regulated by SAUR proteins. Further investigations will be needed to clarify whether SAUR proteins are involved in the regulation of phosphorylation status of PM H^+-ATPase in guard cells. In addition, the identification and characterization of PP2C.D6 and PP2C.D9 interacting proteins in guard cells would provide important insights for regulation of PM H^+-ATPase in guard cells.

Materials and methods

Plant materials and growth conditions

Plants of Arabidopsis (*A. thaliana*) Columbia-0 (Col-0) were used as the wild-type. Col-0 is a background ecotype of T-DNA insertion mutants of *pp2c.d6* (SAIL_171H03), *pp2c.d8* (SALK_143298), and *pp2c.d9* (SALK_026300). These mutants were obtained from the Arabidopsis Biological Resource Center (Ohio State University). All plants were grown on soil under white light (~50 μmol m^{-2} s^{-1}) with a 16-/8-h light/dark cycle in a growth room. Growth temperature and relative humidity were ~20°C–24°C and 40%–60%, respectively.

Transient *PP2Cs* expression assays using Arabidopsis MCPs

To analyze the effect of PP2Cs on the dephosphorylation of PM H^+-ATPase, we constructed the vector carrying *GFP-PP2Cs* under the control of the *35S* promoter. The full-length cDNA of *PP2Cs*, except for *PP2C.D9*, were amplified by PCR and were cloned into *CaMV35S-sGFP(S65T)-NOS3′* vector using In-Fusion HD Cloning Kit (Clontech). The full-length cDNA of *PP2C.D9* was amplified by PCR and was cloned into the BsrGI site of *CaMV35S-sGFP(S65T)-NOS3′* vector. Primers used for the amplification of *PP2Cs* and linearization of the vector were listed in Supplemental Table S2. The resulting constructs (*35S:GFP-PP2Cs:nosT*) were used for transfection into Arabidopsis MCPs. MCPs were isolated as described previously (Wu et al., 2009). Thirty micrograms protoplasts were transfected with 10–20 μg *35S:GFP-PP2Cs:nosT* using the PEG-mediated method (Yoo et al., 2007). After transfections, protoplasts were incubated in incubation buffer (2-mM Mes-KOH, pH 5.7, 0.4-M mannitol, 20-mM KCl, 1-mM $CaCl_2$) for 14 h at room temperature. Protoplasts were harvested by centrifugation at 13,000*g* for 1 min, and cells were lysed in sodium dodecyl sulphate–polyacrylamide gel electrophoresis (SDS–PAGE) sample buffer (15-mM Tris–HCl, pH 8.0, 1.5% [w/v] SDS, 1.5-mM EDTA, 15% [w/v] sucrose, 0.06% [w/v] Coomassie Brilliant Blue, 7.5% [v/v] 2-mercaptoethanol).

Immunoblot

The amount of PM H^+-ATPases and the phosphorylation status of the penultimate Thr residue were detected by immunoblot analysis using specific antibodies against the catalytic domain of AHA2 (anti-H^+-ATPase antibody) and phosphorylated Thr-947 in AHA2 (anti-$pThr_{947}$ antibody; Hayashi et al., 2010). A goat anti-rabbit IgG conjugated to horseradish peroxidase (Bio-Rad Laboratories) was used as a secondary antibody, and the chemiluminescence from the horseradish peroxidase reaction with a chemiluminescence substrate (Thermo Scientific) was detected using the Light Capture AE-2150 system (ATTO). To detect GFP-tagged PP2Cs, mouse anti-GFP antibody (Roche Applied Science) was used as a primary antibody. To detect His-tagged PP2C.D9, mouse anti-His antibody (GE Healthcare) was used as a primary antibody. A goat anti-mouse IgG conjugated to horseradish peroxidase (Bio-Rad Laboratories) was used as a secondary antibody. The chemiluminescent signal was determined using ImageJ software. The phosphorylation level of PM H^+-ATPase was quantified as the ratio of the signal intensity from the phosphorylated PM H^+-ATPase to that from the amount of PM H^+-ATPase. The reduction of the phosphorylation level of PM H^+-ATPase per expression level of PP2Cs was calculated with the following formula:

Reduction of phosphorylation level of PM H^+-ATPase = ([Phosphorylation level of PM H^+-ATPase in GFP expressed MCPs]) – ([Phosphorylation level of PM H^+-ATPase in GFP-tagged PP2C expressed MCPs])/([Signal intensity of GFP in GFP-tagged PP2C expressed MCPs*]/[Signal intensity of GFP in GFP expressed MCPs])

*Signal intensity was quantified from upper band.

Promoter-GUS assay

pro:PP2C.D6::PP2C.D6-GUS, *pro:PP2C.D8::PP2C.D8-GUS*, and *pro:PP2C.D9::PP2C.D9-GUS* transgenic lines (Ren et al., 2018) were used for GUS staining. The GUS staining was performed as reported previously with some modifications (Jefferson et al., 1987). The epidermal tissues from the 4-week-old plants were fixed by 90% acetone for 30 min on ice, and then incubated in distilled water for 10 min. The fixed sample was then incubated in the GUS staining buffer {0.05% (w/v) 5-bromo-5-chloro-3-indolyl-β-D-glucuronide (X-Gluc), 3-mM K5[Fe(CN)6], 3-mM K3[Fe(CN)6], 10-mM EDTA, 0.1% (v/v) Triton X-100, 100-mM sodium phosphate buffer (pH 7.0)} at 37°C for 16 h. After incubation, the sample was washed with 70% (v/v) ethanol. The images of GUS staining were obtained using an upright microscope (Eclipse 50i; Nikon) and a charge-coupled device camera (DS-5Mc-L2; Nikon).

Subcellular localization of PP2C.D6, PP2C.D8, and PP2C.D9

To analyze the subcellular localization of PP2C.D6, PP2C.D8, and PP2C.D9 in guard cells, GFP-fused PP2C.D6, PP2C.D8, and PP2C.D9 proteins were transiently expressed in guard cells of broad bean (*Vicia faba*). Constructions of GFP-fused *PP2C.D6*, *PP2C.D8*, and *PP2C.D9* under control of 35S promoter (*35S:GFP-PP2C.D6:nosT*, *35S:GFP-PP2C.D8:nosT*, and *35S:GFP-PP2C.D9:nosT*) were described above. The constructs or empty vector were introduced into abaxial side of broad bean leaves by particle bombardment (IDERA GIE-III; Tanaka) as described previously (Takemiya et al., 2006). After infection, the leaves were incubated at room temperature in the dark for 16 h. Epidermal strips were peeled and used for microscopic observation. Fluorescent images were obtained with a confocal laser-scanning fluorescent microscopy (FV10i; Olympus).

Construction and observation of transgenic plant *pGC1:GFP-PP2C.D9*

GFP-PP2C.D9 was amplified from *35S:GFP-PP2C.D9:nosT* with specific primers listed in Supplemental Table S3 and cloned into *pPZP211-GC1* vector (Kinoshita et al., 2011; Wang et al., 2014) using BamHI. The resulting construct (*pGC1:GFP-PP2C.D9:nosT*) was introduced into *Agrobacterium tumefaciens* (GV3101). *Agrobacterium* was transformed into Col-0 using floral Dip method as previously described (Kinoshita et al., 2011). F3 homozygous plants were used for the experiments.

For FM4–64 staining, epidermal tissues of rosette leaves from 5-week-old plants were incubated in 2 mL of distilled water containing 10-μM FM4–64 for 15 min at room temperature. Stained samples were washed twice with water and observed by confocal laser scanning microscopy (FV4000; Olympus). Fluorescent images of GFP-PP2C.D9 were obtained with a confocal laser-scanning fluorescent microscopy (FV4000; Olympus). Fluorescence derived from GFP and FM4–64 was exited using 515-nm laser light, and detected using windows ranged from 520 to 550 nm for GFP and from 630 to 670 nm for FM4–64 fluorescence.

RT–PCR

The expression of *PP2C.D6*, *PP2C.D8*, and *PP2C.D9* in the T-DNA insertional mutants was determined by RT–PCR. Total RNA was extracted from rosette leaves of 4-week-old plants using an RNeasy Plant Mini Kit (Qiagen), according to the manufacturer's instructions. First-strand cDNAs were synthesized from the RNA using a Takara PrimeScript II First Strand cDNA Synthesis Kit (Takara) with oligo(dT)12–18 primer. The cDNA fragments were amplified by PCR using specific primers as listed in Supplemental Table S4. *TUB2* (At5g62690) was amplified by RT–PCR to serve as an internal standard.

Measurement of stomatal aperture

Stomatal aperture in epidermal tissues was measured as described previously (Kinoshita et al., 2001; Inoue et al., 2008) with minor modifications. Four- to 5-week-old plants were used for measurement of stomatal aperture. Fully expanded rosette leaves were harvested from dark-adapted plants, at least five plants in each experiment. The leaves were blended in a Waring blender (Waring Commercial) in 35 mL of MilliQ water. The epidermal fragments were collected on a nylon mesh and rinsed with MilliQ water. The epidermal tissues were incubated in basal buffer (5-mM MES-Bistrispropane, 50-mM KCl, and 0.1-mM $CaCl_2$, pH 6.5) and were irradiated with red/blue mixed light (blue light [Stick-B-32; EYELA, Tokyo, Japan] at 10 μmol m^{-2} s^{-1} superimposed on background red light [LED-R; EYELA] at 50 μmol m^{-2} s^{-1}) at 24°C or kept in the dark for 3 h. Stomatal apertures were measured microscopically in the abaxial epidermis by focusing on the inner lips of stomata. In each independent experiment, we measured 30 stomatal apertures in the abaxial epidermis (five stomata per epidermal fragment). All measurements of stomatal response to light were performed between 12:00 p.m. and 2:00 p.m.

Stomatal aperture in leaf discs was measured as described previously (Toh et al., 2018) with modifications. Prior to the measurement, 4- to 5-week-old plants were incubated in the dark overnight. Under dim light, 3-mm diameter leaf discs were excised from fully expanded leaves using a hole punch (Biopsy Punch, Kai Medical). The leaf discs were incubated in the basal buffer in the dark for 3 h. Image of leaf discs were acquired using an optical microscope (BX43; Olympus) with a charge-coupled device camera (DP27; Olympus) with a 20× objective lens (UPlanFL N; Olympus) with the extended focus imaging function of cellSens standard software (Olympus). Stomatal aperture in the abaxial epidermis was quantified from the image of leaf discs using ImageJ software (http://imagej.nih.gov/ij/).

Measurement of stomatal conductance

Stomatal conductance of intact leaves was measured by LI-6400 gas-exchange measurement system (LI-COR) as described previously (Wang et al., 2014). Red light (550 μmol m^{-2} s^{-1}) and blue light (5 μmol m^{-2} s^{-1}) were obtained by halogen projector lamp (power supply: MHAB-150W, Moritex; lamp: Type 6423, PHILIPS) with red and blue filters (red: 2-61; blue: 5-60; Corning), respectively. Flow rate, leaf temperature, and ambient CO_2 concentration were kept at 500 μmol s^{-1}, 23°C, and 400 μmol mol^{-1}, respectively. Relative humidity was 40%–60%. Data represent means of three independent plants with standard error (SE).

Immunohistochemical detection of the PM H^+-ATPase in guard cells

Detections of the phosphorylation level of penultimate residue, Thr, and the amount of PM H^+-ATPase in guard cells were performed using epidermal tissues from Arabidopsis according to a previous method (Hayashi et al., 2011). In brief, the epidermal fragments prepared by blending rosette leaves from 4- to 5-week-old plants were incubated under background red light (50 μmol m^{-2} s^{-1}) for 20 min, after which blue light (10 μmol m^{-2} s^{-1}) was superimposed on the red light for 2.5 min. For time course experiments, red light illumination was continued after blue light pulse (10 μmol m^{-2} s^{-1}, 30 s) and the epidermal tissues were fixed at the indicated time point.

To investigate the effect of exogenous auxin, the epidermal fragments isolated from leaves of dark-adapted plants were incubated with 10-μM IAA, 10-μM FC, or 0.25% (v/v) DMSO (solvent control) for 20 min in the dark. Phosphorylation status of PM H^+-ATPase and the amount of PM H^+-ATPase were detected by anti-$pThr_{947}$ antibody and anti-H^+-ATPase antibody, respectively. The fluorescence from Alexa Fluor488-labeled secondary antibodies was imaged with a fluorescence microscope. The fluorescent signal intensities were quantified using ImageJ software (http://imagej.nih.gov/ij/) as described previously (Hayashi et al., 2011).

In vitro phosphatase assay using recombinant PP2C.D9 protein for the dephosphorylation of yeast-expressed PM H^+-ATPase (AHA2)

The substrate of in vitro phosphatase assay, PM H^+-ATPase (AHA2) was expressed in yeast and was obtained as suspension of microsomal membrane fraction. The full-length cDNA of *AHA2* was amplified by PCR using specific primers listed in Supplemental Table S5 and cloned into the *Bam*HI site of pYES2 vector (Invitrogen). The resulting construct was transformed into *Saccharomyces cerevisiae* strain INVSc1 (*MATa his3D1 leu2 trp1-289 ura3-52*; Invitrogen). Transformed yeast was grown at 28°C for 16 h in preculture medium lacking uracil (0.67% [w/v] yeast nitrogen base, 2% [w/v] glucose, 0.01% [w/v] adenine, arginine, cysteine, leucine, lysine, Thr, tryptophan, 0.05% [w/v] aspartic acid, histidine, isoleucine, methionine, phenylalanine, proline, serine, tyrosine, valine), then transferred to the galactose-containing induction medium (0.67% [w/v] yeast nitrogen base, 2% [w/v] galactose, 1% [w/v] raffinose, 0.01% [w/v] adenine, arginine, cysteine, leucine, lysine, Thr, tryptophan, 0.05% [w/v] aspartic acid, histidine, isoleucine, methionine, phenylalanine, proline, serine, tyrosine, valine) to induce the expression of *AHA2* in the yeast. After induction at 28°C for 16 h, cells were harvested by centrifugation at 1,100*g* for 5 min and resuspended in homogenization buffer (50-mM MOPS-KOH, pH 7.5, 100-mM NaCl, 2.5-mM EDTA, 2-mM DTT, 1-mM PMSF, 20-μM Leupeptine). Suspended cells were homogenized using TissueLyser II (Qiagen) with glass beads (500 μm, Yasui Kikai) at 25.0 Hz for 5 min. The homogenate was centrifuged at 8,000*g* at 4°C for 2 min. The supernatant was further centrifuged at 100,000*g* at 4°C for 1 h. The obtained microsomal membrane fraction, including PM and internal membrane where AHA2 localizes (Jahn et al., 2002), was suspended in resuspension buffer (0.3-M sucrose, 5-mM 2-[4-(2-Hydroxyethyl)-1-piperazinyl]ethanesulfonic acid-Bis-tris propan (HEPES-BTP), pH 7.0, 0.1-M DTT, 1-mM PMSF, 20-μM Leupeptine) and immediately frozen with liquid N_2 and stored under −80°C until use.

Recombinant PP2C.D9 was expressed in *E. coli* and purified. The full-length cDNA of *PP2C.D9* was amplified by PCR using specific primers listed in Supplemental Table S5 and cloned into the BamHI site of pET30a vector (Merck Millipore) using In-Fusion HD Cloning Kit (Clontech; *pET-PP2C.D9*). The resulting construct was transformed into *E.coli* BL21 (DE3) strain. The recombinant PP2C.D9 protein was expressed as N-terminal His-tagged protein (His-PP2C.D9). The fusion protein was purified using Profinity IMAC Ni-Charged Resin (Bio-Rad). The purified His-PP2C.D9 was kept on ice until use.

The yeast microsomal membranes (8-μg protein) were suspended in 25 μL of basal reaction buffer (50-mM MOPS-KOH, pH 7.2, 2.5-mM $MgCl_2$, 1-mM DTT, and 0.025% [w/v] Triton X-100) with or without 0.8-μg protein of recombinant His-PP2C.D9. The dephosphorylation reactions were performed for 30 min at 24°C. The reactions were terminated by solubilization of proteins with SDS–PAGE sample buffer. Phosphorylation status and amount of PM H^+-ATPase was determined using immunoblotting as described above.

Accession numbers

Sequence data from this article can be found in the GenBank/EMBL data libraries under the following accession numbers: *PP2C.D1* (At5g02760), *PP2C.D2* (At3g17090), *PP2C.D3* (At3g12620), *PP2C.D4* (At3g55050), *PP2C.D5* (At4g38520), *PP2C.D6* (At3g51370), *PP2C.D7* (At5g66080), *PP2C.D8* (At4g33920), *PP2C.D9* (At5g06750), *PP2C.A8* (At4g26080), *PP2C.B2* (At2g40180), *PP2C.C4* (At1g07630), *PP2C.E1* (At1g03590), *PP2C.F4* (At1g22280), *PP2C.G1* (At3g62260), *PP2C.H1* (At1g09160), *PP2C.I1* (At2g25070), *AHA2* (At4g30190), *SAUR9* (At4g36110), *SAUR19* (At4G36110), and *TUB2* (At5g62690).

Supplemental data

The following materials are available in the online version of this article.

Supplemental Figure S1. Effect of transiently expressed PP2C.A-Is on phosphorylation status of PM H^+-ATPase in MCPs.

Supplemental Figure S2. Expression level of *PP2C.D6* and *PP2C.D9* in guard cells and mesophyll cells.

Supplemental Figure S3. Subcellular localization of GFP-PP2C.D9 fusion proteins in guard cells.

Supplemental Figure S4. Immunohistochemical detection of guard-cell PM H^+-ATPase in Col-0, *pp2c.d6*, *pp2c.d9*, and *pp2c.d6/9* double mutant.

Supplemental Figure S5. Immunohistochemical detection of guard-cell PM H^+-ATPase in Col-0 and *pp2c.d6/9* during time course experiment.

Supplemental Figure S6. Time course of light-dependent changes in stomatal conductance in intact leaves from Col-0 and *pp2c.d6/9*.

Supplemental Figure S7. Stomatal aperture of leaf discs from Col-0 and *pp2c.d6/9* incubated in the dark.

Supplemental Figure S8. Expression of *PP2C.Ds* in 4-d-old seedlings.

Supplemental Table S1. Expression level of *PP2C.Ds* in GCPs.

Supplemental Table S2. List of primers for construction of *35S:GFP-PP2Cs:nosT*.

Supplemental Table S3. List of primers for construction of *pPZP211-pGC1:GFP-PP2C.D9*.

Supplemental Table S4. List of primers for RT-PCR.

Supplemental Table S5. List of primers for constructions used for *in vitro* phosphatase assay.

Funding

This work was supported by Grants-in-Aid for Scientific Research from the Ministry of Education, Culture, Sports, Science, and Technology, Japan (grant nos. 20H05687 and 20H05910 to T.K.), by Technology of Japan and from the Advanced Low Carbon Technology Research and Development Program from the Japan Science and Technology Agency (JPMJAL1011 to T.K.), the National Science Foundation (MCB-1613809 to W.M.G.), and the National Institutes of Health (GM067203 to W.M.G.).

Conflict of interest statement. None declared.

References

Ando E, Kinoshita T (2018) Red light-induced phosphorylation of plasma membrane H^+-ATPase in stomatal guard cells. Plant Physiol **178**: 838–849

Aoki S, Toh S, Nakamichi N, Hayashi Y, Wang, Y, Suzuki T, Tsuji H, Kinoshita T (2019) Regulation of stomatal opening and histone modification by photoperiod in *Arabidopsis thaliana*. Sci Rep **9**: 10054

Doi M, Shigenaga A, Emi T, Kinoshita T, Shimazaki K (2004) A transgene encoding a blue-light receptor, phot1, restores blue-light responses in the Arabidopsis phot1 phot2 double mutant. J Exp Bot **55**: 517–523.

Falhof J, Pedersen JT, Fuglsang AT, Palmgren M (2016) Plasma membrane H^+-ATPase regulation in the center of plant physiology. Mol Plant **9**: 323–337

Haruta M, Gray WM, Sussman MR (2015) Regulation of the plasma membrane proton pump (H^+-ATPase) by phosphorylation. Curr Opin Plant Biol **28**: 68–75

Hayashi M, Inoue S, Takahashi K, Kinoshita T (2011) Immunohistochemical detection of blue light-induced phosphorylation of the plasma membrane H^+-ATPase in stomatal guard cells. Plant Cell Physiol **52**: 1238–1248

Hayashi M, Inoue S, Ueno Y, Kinoshita T (2017) A Raf-like protein kinase BHP mediates blue light-dependent stomatal opening. Sci Rep **7**: 45586

Hayashi Y, Nakamura S, Takemiya A, Takahashi Y, Shimazaki K, Kinoshita T (2010). Biochemical characterization of *in vitro* phosphorylation and dephosphorylation of the plasma membrane H^+-ATPase. Plant Cell Physiol **51**: 1186–1196

Hayashi Y, Takahashi K, Inoue S, Kinoshita T (2014) Abscisic acid suppresses hypocotyl elongation by dephosphorylating plasma membrane H^+-ATPase in *Arabidopsis thaliana*. Plant Cell Physiol **55**: 845–853

Inoue S, Kinoshita T, Matsumoto M, Nakayama K, Doi M, Shimazaki K (2008) Blue light-induced autophoshporylation of phototropin is a primary step for signaling. Proc Natl Acad Sci USA **105**: 5626–5631

Inoue S, Kinoshita T (2017) Blue light regulation of stomatal opening and the plasma membrane H^+-ATPase. Plant Physiol **174**: 531–538

Jahn TP, Schulz A, Taipalensuu J, Palmgren MG (2002) Post-translational modification of plant plasma membrane H^+-ATPase as a requirement for functional complementation of a yeast transport mutant. J Biol Chem **277**: 6353–6358

Jefferson RA, Kavanagh TA, Bevan MW (1987) GUS fusions: beta-glucuronidase as a sensitive and versatile gene fusion marker in higher plants. EMBO J **6**: 3901–3907

Kinoshita T, Shimazaki K (1999) Blue light activates the plasma membrane H^+-ATPase by phosphorylation of the C-terminus in stomatal guard cells. EMBO J **18**: 5548–5558

Kinoshita T, Doi M, Suetsugu N, Kagawa T, Wada M, Shimazaki K (2001) phot1 and phot2 mediate blue light regulation of stomatal opening. Nature **414**: 656–660

Kinoshita T, Shimazaki K (2001) Analysis of the phosphorylation level in guard-cell plasma membrane H^+-ATPase in response to fusicoccin. Plant Cell Physiol **42**: 424–432

Kinoshita T, Ono N, Hayashi Y, Morimoto S, Nakamura S, Soda M, Kato Y, Ohnishi M, Nakano T, Inoue S, et al. (2011) *FLOWERING LOCUS T* regulates stomatal opening. Curr Biol **21**: 1232–1238

Lohse G, Hedrich R (1992) Characterization of the plasma-membrane H^+-ATPase from *Vicia faba* guard cells. Planta **188**: 206–214

Maudoux O, Batoko H, Oecking C, Gevaert K, Vandekerckhove, J, Boutry M, Morsomme P (2000) A plant plasma membrane H^+-ATPase expressed in yeast is activated by phosphorylation at its penultimate residue and binding of 14-3-3 regulatory proteins in the absence of fusicoccin. J Biol Chem **275**: 17762–17770

Minami A, Takahashi K, Inoue S, Tada Y, Kinoshita T (2019) Brassinosteroid induces phosphorylation of the plasma membrane H^+-ATPase during hypocotyl elongation in *Arabidopsis thaliana*. Plant Cell Physiol **60**: 935–944

Palmgren MG (2001) Plant plasma membrane H^+-ATPase: powerhouses for nutrient uptake. Annu Rev Plant Physiol Plant Mol Biol **52**: 817–845

Ren H, Gray WM (2015) SAUR proteins as effectors of hormonal and environmental signals in plant growth. Mol Plant **8**: 1153–1164

Ren H, Park MY, Spartz AK, Wong JH, Gray WM (2018) A subset of plasma membrane-localized PP2C.D phosphatases negatively regulate SAUR-mediated cell expansion in Arabidopsis. PLoS Genet **14**: e1007455

Schweighofer A, Hirt H, Meskiene I (2004) Plant PP2C phosphatases: emerging functions in stress signaling. Trends in Plant Sci **9**: 236–243

Shimazaki K, Doi M, Assmann SM, Kinoshita T (2007) Light regulation of stomatal movement. Annu Rev Plant Biol **58**: 219–247

Sondergaard TE, Schulz A, Palmgren MG (2004). Energization of transport processes in plants. roles of the plasma membrane H^+-ATPase. Plant Physiol **136**: 2475–2482

Spartz AK, Ren H, Park MY, Grandt KN, Lee SH, Murphy AS, Sussman MR, Overvoorde PJ, Gray WM (2014) SAUR inhibition of PP2C-D phosphatases activates plasma membrane H^+-ATPases to promote cell expansion in *Arabidopsis*. Plant Cell **26**: 2129–2142

Spartz AK, Lor VS, Ren H, Olszewski NE, Miller ND, Wu G, Spalding EP, Gray WM (2017) Constitutive expression of Arabidopsis SMALL AUXIN UP RNA19 (SAUR19) in Tomato confers auxin-independent hypocotyl elongation. Plant Physiol **173**: 1453–1462

Sun N, Wang J, Gao Z, Dong J, He H, Terzaghi W, Wei N, Deng XW, Chen H (2016) Arabidopsis SAURs are critical for differential light regulation of the development of various organs. Proc Natl Acad Sci USA **113**: 6071–6076

Svennelid F, Olsson A, Piotrowski M, Rosenquist M, Ottman C, Larsson C, Oecking C, Sommarin M (1999) Phosphorylation of Thr-948 at the C terminus of the plasma membrane H^+-ATPase creates a binding site for the regulatory 14-3-3 protein. Plant Cell **11**: 2379–2391

Takahashi K, Hayashi K, Kinoshita T (2012) Auxin activates the plasma membrane H^+-ATPase by phosphorylation during hypocotyl elongation in *Arabidopsis thaliana*. Plant Physiol **159**: 632–641

Takemiya A, Kinoshita T, Asanuma M, Shimazaki K (2006) Protein phosphatase 1 positively regulates stomatal opening in response to blue light in *Vicia faba*. Proc Natl Acad Sci USA **103**: 13549–13554

Takemiya, A, Sugiyama N, Fujimoto H, Tsutsumi T, Yamauchi S, Hiyama A, Tada Y, Christie JM, Shimazaki K (2013) Phosphorylation of BLUS1 kinase by phototropins is a primary step in stomatal opening. Nat Commun **4**: 2094

Tanaka Y, Sano T, Tamaoki M, Nakajima N, Kondo N, Hasezawa S (2006) Cytokinin and auxin inhibit abscisic acid-induced stomatal closure by enhancing ethylene production in *Arabidopsis*. J Exp Bot **57**: 2259–2266

Toda Y, Wang Y, Takahashi A, Kawai Y, Tada Y, Yamaji N, Ma JF, Ashikari M, Kinoshita T (2016) *Oryza sativa* H^+-ATPase (OSA) is involved in the regulation of dumbbell-shaped guard cells of rice. Plant Cell Physiol **57**: 1220–1230

Toh S, Inoue S, Toda Y, Yuki T, Suzuki K, Hamamoto S, Fukatsu K, Aoki S, Uchida M, Asai E, et al. (2018) Identification and characterization of compounds that affect stomatal movements. Plant Cell Physiol **59**: 1568–1580

Tovar-Mendez A, Ján A. Miernyk JA, Hoyos E, Randall DD (2014) A functional genomic analysis of Arabidopsis thaliana PP2C clade D. Protoplasma **251**: 265–271

Uchida N, Takahashi K, Iwasaki R, Yamada R, Yoshimura M, Endo TA, Kimura S, Zhang H, Nomoto M, Tada Y, et al. (2018) Chemical hijacking of auxin signaling with an engineered auxin-TIR1 pair. Nat Chem Biol **14**: 299–305

Ueno K, Kinoshita T, Inoue S, Emi T, Shimazaki K (2005) Biochemical characterization of plasma membrane H^+-ATPase activation in guard cell protoplasts of *Arabidopsis thaliana* in response to blue light. Plant Cell Physiol **46**: 955–963

Wang Y, Noguchi K, Ono N, Inoue S, Terashima I, Kinoshita T (2014) Overexpression of plasma membrane H^+-ATPase in guard cells promotes light-induced stomatal opening and enhances plant growth. Proc Natl Acad Sci USA **111**: 533–538

Winter D, Vinegar B, Nahal H, Ammar R, Wilson GV, Provart NJ (2007) An "Electronic Fluorescent Pictograph" browser for exploring and analyzing large-scale biological data sets. PLoS One **28**: e718

Wong JH, Angela K. Spartz AK, Park MY, Du M, Gray WM (2019) Mutation of a conserved motif of PP2C.D phosphatases confers SAUR immunity and constitutive activity. Plant Physiol **181**: 353–366

Wong JH, Klejchova M, Snipes SA, Nagpal P, Bak G, Wang B, Dunlap S, Park MY, Kunkel EN, Trinidad B, et al. (2021) SAUR proteins and PP2C.D phosphatases regulate H^+-AT Pases and K+ channels to control stomatal movements. Plant Physiol **185**: 256–273

Wu FH, Shen SC, Lee LY, Lee SH, Chan MT, Lin CS (2009) Tape-Arabidopsis sandwich – a simpler Arabidopsis protoplast isolation method. Plant Methods **5**: 16

Xue T, Wang D, Zhang S, Ehlting J, Ni F, Jakab S, Zheng C, Zhong Y (2008) Genome-wide and expression analysis of protein phosphatase 2C in rice and Arabidopsis. BMC Genomics **9**: 550

Yamauchi S, Takemiya A, Sakamoto T, Kurata T, Tsutsumi T, Kinoshita T, Shimazaki K (2016) The plasma membrane H^+-ATPase AHA1 plays a major role in stomatal opening in response to blue light. Plant Physiol **171**: 2731–2743

Yang Y, Costa A, Leonhardt N, Siegel RS, Schroeder JI (2008). Isolation of a strong Arabidopsis guard cell promoter and its potential as a research tool. Plant Methods **4**: 6

Yoo SD, Cho YH, Sheen J (2007) Arabidopsis mesophyll protoplasts: a versatile cell system for transient gene expression analysis. Nat Protoc **2**: 1565–1572